Preprints (www.preprints.org) | NOT PEER-REVIEWED | Posted: 24 November 2020 doi:10.20944/preprints202011.0608.v1

Article

The Impact of Utility-Scale Photovoltaics Plant on Near Surface Turbulence Characteristics in Gobi areas

Junxia Jiang[1,2], Xiaoqing Gao[1*], Bolong Chen[3]

[1] Key Laboratory of Land Surface Process and Climate Change in Cold and Arid Regions, Northwest Institute of Eco-Environment and Resources, Chinese Academy of Sciences, Lanzhou, Gansu 730000, China

[2] University of Chinese Academy of Sciences, Beijing 100049, China

[3] Key Laboratory for Semi-Arid Climate Change of PRC Ministry of Education, College of Atmospheric Sciences, Lanzhou University, Lanzhou 730000, China

Correspondence: xqgao@lzb.ac.cn

Abstract: The local climate effects of utility-scale photovoltaic (PV) plants have also attracted more and more attention with the rapid development of PV industry. Turbulent fluxes and intensity characteristics for the PV plant and the adjacent reference site are investigated in the gobi areain Wujianqu in Xinjiang. Results indicate that near surface boundary layer is more unstable during the daytime while is more stable at the night in the PV plant than the reference site. The average roughness is 0.089m and 0.041m for the PV plant and the reference site respectively. The turbulence intensity in the vertical direction (I_w) of the PV plant is higher than the reference site especially during the daytime. The turbulent kinetic energy of the PV plant during the daytime is lower than the reference site.The momentum in the PV plant is higher than the reference site, especially during the daytime. Compared to the reference site, the PV plant has higher sensible heat flux and less latent heat flux. Site specific turbulent intensity relationships were developed for the PV plant and the reference site by analyzing wind components as a function of stability parameter (z/L). The turbulent components of wind followed 1/3 power law in the unstable conditions and stable conditions in the PV plant and the reference site.

Keywords: large-scale photovoltaic plants; M-O similarity theory; roughness; stability; turbulence intensity

1. Introduction

For a long time, people have realized that the excessive consumption of traditional fossil fuels not only accelerates the rate of reduction of fossil fuel reserves, but also leads to increased health risks and threats to global climate change, causing significant adverse effects on the global environment [1]. A feasible solution against the problem is represented by the generation of electricity from sunlight [2]. The rapid progress of photovoltaic(PV) technologies and dramatic reduction of cost has impelled the development of PV industry[3,4]. Compared with traditional energy sources, PV generation has potential to reduce pollutant emissions and reclaim degraded land [5,6]. However, the widespread deployment of large-scale PV panels require a large amount of land and have

© 2020 by the author(s). Distributed under a Creative Commons CC BY license.

Preprints (www.preprints.org) | NOT PEER-REVIEWED | Posted: 24 November 2020 doi:10.20944/preprints202011.0608.v1

potential to influence the regional and local climate through change the radiative (albedo) and non-radiative (surface roughness and Bowen ratio) surface biophysical properties [7,8].

In the previous studies, some simulation and field observation found that utility-scale solar energy infrastructure in the barren areas produce a heating effect about 2~4K on the near surface air through the operation process due to low albedo and specific heat capacity of PV panels [9-11]. The PV panels have a cooling effect up to 6K on surface soil during the daytime due to physical shielding while have a warming effect more than 2K on surface soil in the nighttime due to hindering of long wave radiation cooling [11,12]. Furthermore, numerical modeling showed that large deployment of PV panels in the desert can trigger the positive feedback of albedo-precipitation-vegetation, resulting in an increase of precipitation [13,14]. Recent observations found that PV array increase the sensible heat flux and reduce the storage and release of surface heat flux [15], which reveals the characteristics of radiation balance and energy distribution of the PV plant and provides a reference for further discussing the interaction process between PV arrays and near surface atmosphere.

Despite the effect of large-scale PV applications on local climate was demonstrated in the above-metioned advances, it is unclear that the impact of PV panels on turbulence characteristic. However, the transport of momentum, heat and moisture between the earth's surface and atmosphere is dominated by the characteristics of turbulent exchange, which is the main physical process in the atmospheric boundary layer and considered to play an important role in the formation and evolution of planetary boundary layer and various weather phenomena and the air pollutants diffusion [16-20]. According to the Monin-Obukhov similarity (MOS) theory, the nondimensional wind speed component can be expressed as universal function of the non-dimensional stability parameter under steady and horizontally homogeneous conditions. In recent decades, with the deepening of theoretical research and the progress of observation technology, the verification of the validity of the application of MOS theory over different surface conditions has been carried out. For example, studies found that the relationship between normalized standard deviation of wind speed and the stability parameter on the flat underlying surface accord with 1/3 power law [21]. MOS theory failed to be verified for the coastal maine boundary layer in near-neutral and stable conditions [22]. Studies in the Qinghai-Tibet Plateau show that the relationship between statistics of turbulence and stability oarameter satisfy MOS theory under stable and unstable conditions [23,24]. In addition, the variance of dimensionless velocity component in the surface layer of urban surface changes with stability, which basically satisfies the MOS theory [25,26]. Turbulence intensity in the ocean is mainly controlled by thermal effect, and the statistical characteristics of turbulence in autumn and winter are basically meet MOS theory [27,28].

Conventional, utility-scale solar energy infrastructure modifies turbulence characteristics through the interaction process of panel and atmosphere. Assessing the impacts of PV deployment on turbulence characteristics can helpful to deeply understand the interaction between the PV underlying surface and the near-surface atmosphere and of great significance to understand and capture the impact mechanism of PV panels on the local climate effect in barren areas. Given this, we investigated the characteristics of the near surface atmospheric turbulence and dynamic and thermal properties similar to those at an undisturbed reference site. We carried out the experiment at a utility scale PV plant in Wujiaqu barren area in Xinjiang. This study is presented as follows: Section 2 introduce the experiment design and the derived methodology related to the tubulence parameters discussed in this study; Section 3 presents the comparison results and relevant discussions; Section 4

Preprints (www.preprints.org) | NOT PEER-REVIEWED | Posted: 24 November 2020 doi:10.20944/preprints202011.0608.v1

summarizes the conclusions.

2. Site overview and methods

2.1. Site overview

This experiment took place in a utility scale PV plant in Wujiaqu Gobi area of Xinjiang. Wujiaqu is located at the intersection of the desert and oasis in the southeast of the Jungar Basin. It is cold in winter and hot in summer, and it is dry all year round, belongs to a continental arid climate. The PV array is erected on the underlying of the Gobi with sparse vegetation, with a length of 1120m from north to south and a width of 1030m from east to west, covering an area of about 1.15km^2 and an installed capacity of 70MW. The PV array in the plant faces south and the inclination angle is 37°, the row spacing of the PV array is 7.5m, and the top of the PV panel is about 2.5m above the ground. The panel material is polysilicon and the maximum power is 250W. The location of the observation site in the PV plant is 44.406°N , 87.656°E, and the altitude is 439m. The reference site is located at 910m northeast of the observation point in the plant (44.409°N,87.667°E), and the altitude is 437m. The terrain is relatively flat (Figure. 1). The observation towers of the two sites are both 11m high, and the underlying surfaces are Gobi with sparse vegetation. The soil type is sandy soil and the soil texture is relatively coarse.

(a) (b) (c)

Figure 1. Photos of the monitoring sites for the PV plant (a) and the reference site (c) in the Wujiaqu barren area. The map shows the spatial distribution of the PV plant and the reference site as extracted from Google Earth by the end of 2018 (b).

The various turbulence parameters are derived from the ultrasonic open-circuit vortex covariance system which were installed at the heights of 5.5m and 3m in the PV plant and the reference site respectively. The model of the ultrasonic open-circuit vortex covariance system is IRGASON-IC-BB, produced by Campbell, USA and integrated an open-circuit infrared gas analyzer and a three-dimensional ultrasonic anemometer. The three-dimensional ultrasonic anemometer points to the main wind direction to measure the three-dimensional wind speed and the open-circuit infrared gas analyzer is used to measure the CO_2/H_2O concentration. The eddy correlation system can measure the vertical flux of heat and water vapor in the atmosphere and various pulsation. The data collection and sampling frequency is 10Hz. The data period is from June 8th to October 31st, 2019. The time used in this paper is Beijing time.

2.2. Flux data processing and calculation methods

The original observation of 10Hz ultrasound data is processed by Easyflux online software processing system for post-data processing and quality control, mainly including outlier elimination, double rotation and plane fitting method coordinate rotation[29], frequency delay time correction

Preprints (www.preprints.org) | NOT PEER-REVIEWED | Posted: 24 November 2020 doi:10.20944/preprints202011.0608.v1

[30], ultrasonic virtual temperature correction[31] and WPL correction[32]. The final processing is the average turbulent flux of 30 minutes, and the data quality evaluation such as turbulence stability test and development adequacy ITC test are performed on it.

The surface layer parameters analyzed in this study mainly include friction velocity u_*, temperature scale T_*, stability parameter z/L, roughness length $z0$, turbulence intensity I, turbulent kinetic energy e, momentum flux τ, sensible heat flux H and latent heat flux LE. Normalized standard deviation of 3D wind, temperature and concentration of water vapor and CO2 are analyzed as a function of z/L. The eddy correlation method was employed to derive these parameters.

In the boundary layer, after introducing dimensionless variables through scale parameters, the contours of many variables can be expressed in a general form[33].

Among them, the scaling speed is also called friction speed, which is a basic surface speed scaling parameter, which is obtained by the following formula:

$$u_* = \left(\overline{(u'w')}^2 + \overline{(v'w')}^2\right)^{\frac{1}{4}} \quad (1)$$

The temperature scale and length scale parameters are as follows:

$$T_* = \frac{\overline{w'T'}}{u_*} \quad (2)$$

$$L = \frac{-{u_*}^3\overline{T}}{kg\left(\overline{w'T'}\right)} \quad (3)$$

Among them, the three-dimensional wind speed component and temperature fluctuation are obtained by subtracting the average value from the instantaneous value of each parameter, that is, $u' = u - \overline{u}$, $v' = v - \overline{v}$, $w' = w - \overline{w}$, $T' = T - \overline{T}$, k=0.4 is the Von Karman constant, and g is the acceleration of gravity.

Atmosphere stability parameter z/L is a measure of buoyancy convection ability and is obtained by:

$z/L = \frac{z-d}{L}$ (4)

where z is the measurement height (5.5m for the PV plant and 3m for the reference site), d is the zero-plane displacement.

The roughness length $z0$ depends not only on surface type but also on surface roughness texture and derived from a wind profile under neutral conditions [34]:

$z0 = (z-d)\exp\left(-\frac{k\sqrt{\overline{u}^2+\overline{v}^2}}{u_*}\right)$ (5)

Turbulence intensity is defined as the ratio of the standard deviation of the three wind speed components to the average wind speed:

$$I_u = \sigma_u/\overline{U},\ I_v = \sigma_v/\overline{U},\ I_w = \sigma_w/\overline{U} \quad (6)$$

σ_u、σ_v、σ_w are the standard deviation of wind speed fluctuation:$\sigma_u = \sqrt{\overline{u'u'}}$, $\sigma_v = \sqrt{\overline{v'v'}}$, $\sigma_w = \sqrt{\overline{w'w'}}$.

The turbulent parameters are computed using following formulae.

$e = 0.5(\sigma_u{}^2 + \sigma_v{}^2 + \sigma_w{}^2)$ (7)

$\tau = -\rho\overline{u'w'}$ (8)

$H = C_p\rho\overline{w'T'}$ (9)

$LE = \lambda\rho\overline{w'q'}$ (10)

Preprints (www.preprints.org) | NOT PEER-REVIEWED | Posted: 24 November 2020 doi:10.20944/preprints202011.0608.v1

Where ρ and C_p are the density and the constant specific heat capacity of air, q' is the fluction of water vapor density and λ is the latent heat of evaporation.

The M-O similarity theory is an important basis for understanding and explaining the characteristics of low-level atmospheric turbulence, and the relationship between flux, wind speed and scalar variance can be obtained [35]. According to the M-O similarity theory, the normalized standard deviation of the turbulent velocity component can be expressed by the universal function of the atmospheric stability parameter z/L:

$$\frac{\sigma_{u,v,w}}{u_*} = c_1(1 + c_2|z/L|)^{\frac{1}{3}} \qquad (11)$$

Under the condition of free convection, the dimensionless temperature variance σ_T/|T_* | satisfies the following relationship with the stability z/L:

$$\frac{\sigma_T}{|T_*|} = c(-z/L)^{\frac{1}{3}} \qquad (12)$$

Where c is the site-specific modeling coefficients.

3. Results and discussions

3.1. Atmospheric stability parameter and aerodynamic roughness

Atmospheric stability z/L and aerodynamic roughness $z0$ are important factors that control the energy exchange between the earth and atmosphere. They are the most important physical parameters on the earth's surface and are essential for accurate calculation of the turbulent flux on the earth's surface. The diurnal variation of z/L is analyzed for the PV plant and the reference site in Figure 2. The positive z/L during early morning and at night indicate stable conditions of near-surface atmosphere due to the stratification of atmosphere caused by surface radiational cooling, while the negative z/L during the daytime from 9:00 to 17:00 indicate unstable conditions resulted from the accumulation of surface solar radiation. Although similar characteristics of z/L are found in both sites there are few differences. In the PV plant (Figure 2(a)), the atmosphere is higher unstable with the minimun average of z/L less than -1.5 at 12:00 than the reference site during the daytime. The highly unstable conditions of near surface atmosphere may be caused by the strong convection exchange in the PV plant reported in the previous study [15]. For nocturnal hours, lager z/L for the PV plant indicating more stable near surface atmospheric stratification than that of the reference site. This highly stable condition may be resulted from the thermal insulation effect of PV modules on the ground surface at night[14]. The variability of z/L in the PV plant is larger than that of the reference site as evident from the length of the whiskers.

Aerodynamic roughness $z0$ refers to the height of the ground with a wind speed of zero and changes dynamically because its magnitude not only depends on the structure and shape of the surface roughness element, but also depends on the near-surface airflow conditions to a certain extent [36]. The magnitude of $z0$ in the PV plant is between 0.08 and 0.1m, while in the reference site is slightly larger than 0.04m, and the $z0$ in the PV plant is larger than the reference site and changes more drastic (Figure 2(c)). This is because the PV underlying surface is rougher than the flat barren Gobi surface, and the panels have a greater effect on the airflow, which leads to a larger roughness. For the average roughness, the PV plant and the reference site are 0.089m and 0.041m respectively, which are not much different from the grassland and shrub sandbags in New Mexico[37], but an order of magnitude larger than the Heihe desert(0.0045m), Heihe Gobi(0.0045m) and Dunhuang Gobi (0.0019) which may be related to turbulent conditions near the ground surface.

Preprints (www.preprints.org) | NOT PEER-REVIEWED | Posted: 24 November 2020 doi:10.20944/preprints202011.0608.v1

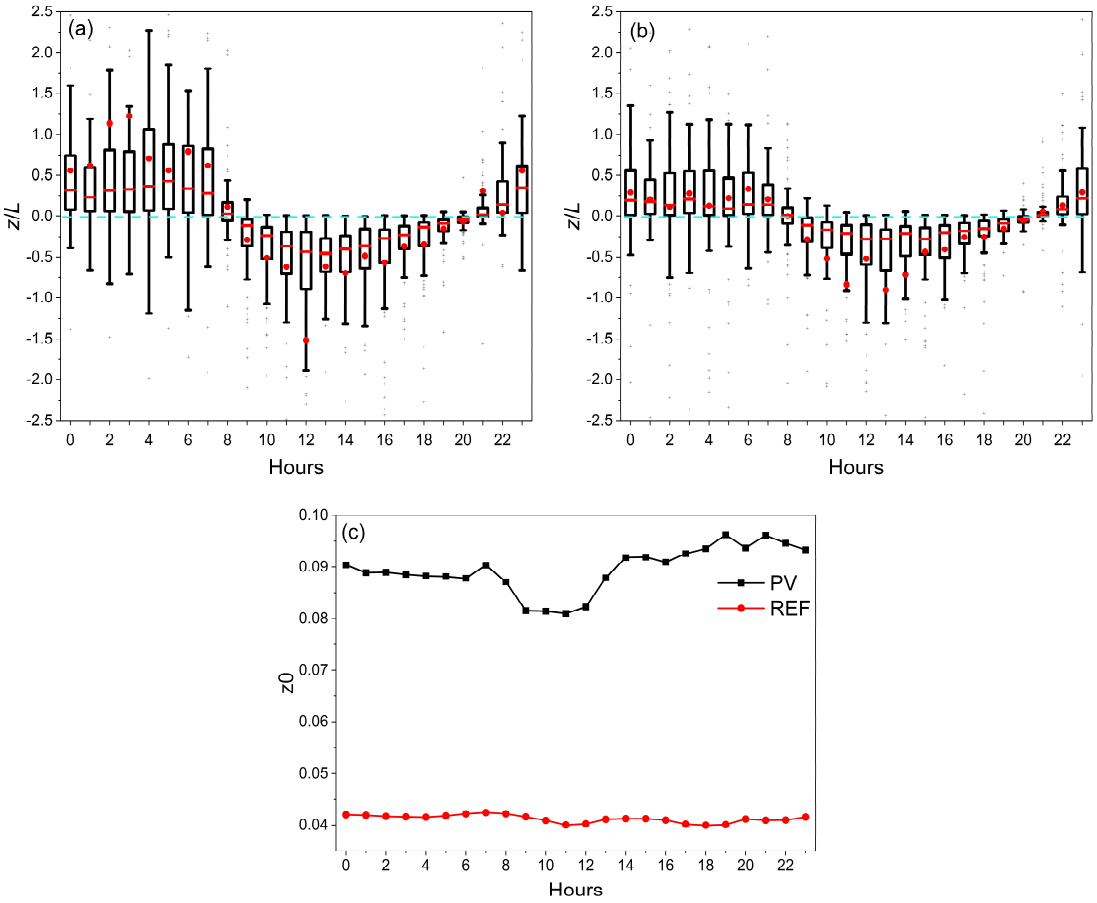

Figure 2. Diurnal variation of the atmospheric stability parameter z/L in the PV plant (a) and the reference site (b) The height of the box shows the range from 25th to 75th percentile. The horizontal red line inside the box and solid red dot denote the median value and mean value respectively. The ends of the whiskers are drawn to 10th and 90th percentile values. (c) is the aerodynamic roughness $z0$ in the PV plant and the reference site

3.2. Scaling parameters

Friction velocity u_* is the main dynamic characteristic parameter that characterizes the interaction between the near-surface airflow and the surface roughness element. As the velocity scale of turbulent motion, it reflects the diffusion and transport capacity in all directions in space [38]. The u_* of the PV site and the reference site have obvious diurnal variations, with large fluctuations during the daytime, and both can reach more than 0.3m/s in the afternoon and stable at the night that keep near 0.1m/s (Figure. 3). The u_* of the PV site is larger than that of the reference site, indicating that the turbulent mixing in the PV plant is more complete. In the entire daily cycle, the friction speed in the PV plant is higher than the reference site, which is not only affected by the difference in surface roughness element, but also related to the wind speed and the intensity of mechanical turbulence. The wind speed of the PV plant decreases faster due to the airflow is blocked by the panels, and the wind speed pulsation is larger than that of the reference site, which is particularly obvious during the daytime.

The characteristic temperature T_* of the PV plant and the reference site have the opposite trend to the u_* (Figure. 3). They begin to decrease at 8:00, and in the afternoon the PV plant and the reference site decrease to -0.65 and -0.47 respectively. Then gradually increase and reach above 0 after 20:00. The u_* is relatively stable at night, maintaining within the range of 0 to 0.1. During the daytime, the PV plant is significantly lower than the reference site, while at night it is slightly higher than the reference site. When the atmospheric stratification tends to be stable, the u_* in the PV plant

Preprints (www.preprints.org) | NOT PEER-REVIEWED | Posted: 24 November 2020 doi:10.20944/preprints202011.0608.v1

and the reference site increase rapidly with the increase of the stability, and both reach the maximum value at the near neutral stratification. The maximum u_* in the PV plant can reach more than 1.2m/s. while the maximum u_* in the reference site is 0.98m/s; when the atmospheric is in an unstable stratification, u_* tends to gradually decrease as the instability increases. T_* is relatively discrete under unstable conditions, and maintains around 0 when the neutral stratification.

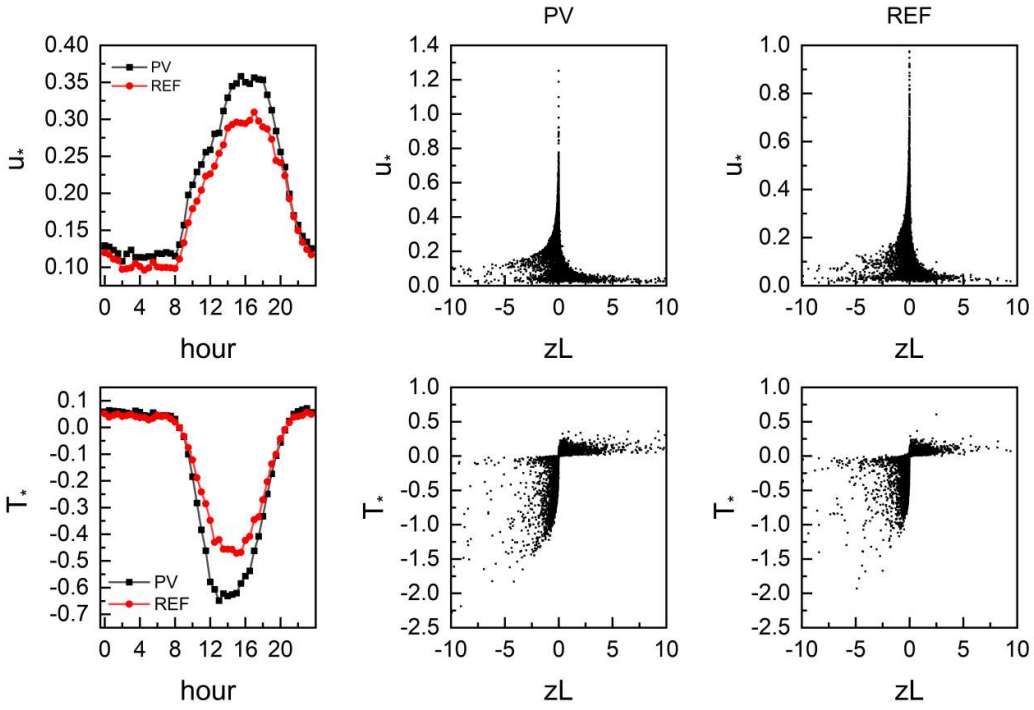

Figure 3. Variation of the scaling parameter of velocity (u_*), temperature (T_*) with time and stability in the PV plant and the reference site

3.3. Turbulence intensity and turbulent kinetic energy

Turbulence intensity characterizes the strength of atmospheric turbulence motion and the magnitude of turbulence motion energy. Comparing the turbulence intensity of the PV plant and the reference site helps to understand the impact of PV panels on the near-surface turbulence characteristics and material energy transport in barren areas. The turbulence intensity components I_u(longitudinal wind), I_v(lateral wind) and I_w(vertical wind) of the three wind directions of the PV plant and the reference site have obvious diurnal variation (Fig. 4). In the unstable condition with strong wind speed and strong heating during the daytime, the turbulence is fully developed and relatively strong. For the horizontal turbulence intensity I_u and I_v, the former of the PV plant is slightly higher than the reference site, and the latter of the reference site is slightly higher than the PV plant. This may be related to the installation direction of the PV panels. The PV panels are placed facing south, which produce greater friction and obstruction to the north-south airflow, making the north-south wind speed decrease more and the longitudinal wind speed pulsation is larger than the reference site, resulting in the stronger longitudinal turbulence intensity. While the air flow in the PV plant is concentrated and divided into the east-west direction, making the wind speed decreases less and the wind speed pulsation is smaller than the reference site, resulting in the weaker lateral turbulence intensity. Convective exchange near the ground is suppressed, and turbulence is mainly generated by mechanical dynamics at night, I_u and I_v of the PV plant are smaller than the reference site mainly induced by the lower wind speed in the PV plant. Regarding the vertical turbulence intensity I_w, most of the time the PV plan is significantly higher than the reference site. This may be due to the blocking effect of the panels in the PV plant. The wind speed decreases more obviously,

Preprints (www.preprints.org) | NOT PEER-REVIEWED | Posted: 24 November 2020 doi:10.20944/preprints202011.0608.v1

and the vertical exchange effect of the atmosphere is also more obvious. The average of I_u, I_v and I_w in the PV plant (the reference site) are 0.29 (0.32), 0.34 (0.34) and 0.12 (0.10), indicating that the turbulence intensity in the horizontal direction is larger than that in the vertical direction, and the turbulence intensity in the horizontal direction is dominant. The turbulence intensity in the horizontal direction of the PV plant is slightly lower than the reference site, while the vertical direction is opposite.

From the variation of turbulence intensity with wind speed (Fig. 5), it can be seen that wind speed affects the development of turbulence. The lower the wind speed, the greater the intensity of turbulence exchange in the three directions. In the state of free convection where the wind speed is less than 2m/s, the turbulence intensity of the PV plant and the reference site decrease rapidly with the increase of wind speed; when the wind speed is less than 4m/s, the turbulence develops vigorously; when the wind speed is greater than 6m/s, the turbulence intensity is both becoming steady. When the wind speed is less than 4m/s, the variation amplitude of the turbulence intensity in the PV plant with the wind speed is smaller than that of the reference site, and the vertical direction is particularly obvious.

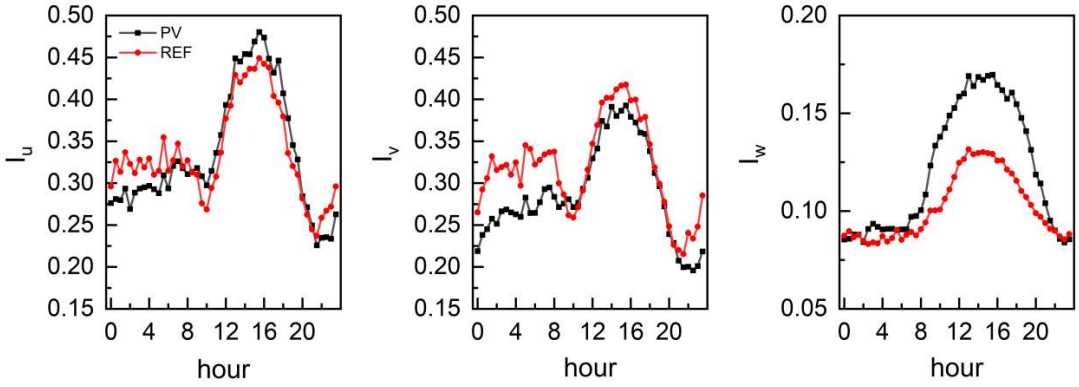

Figure 4. The average daily variation of turbulence intensity component of longitudinal wind (I_u), lateral wind (I_v) and vertical wind (I_w) for the PV plant (the reference site)

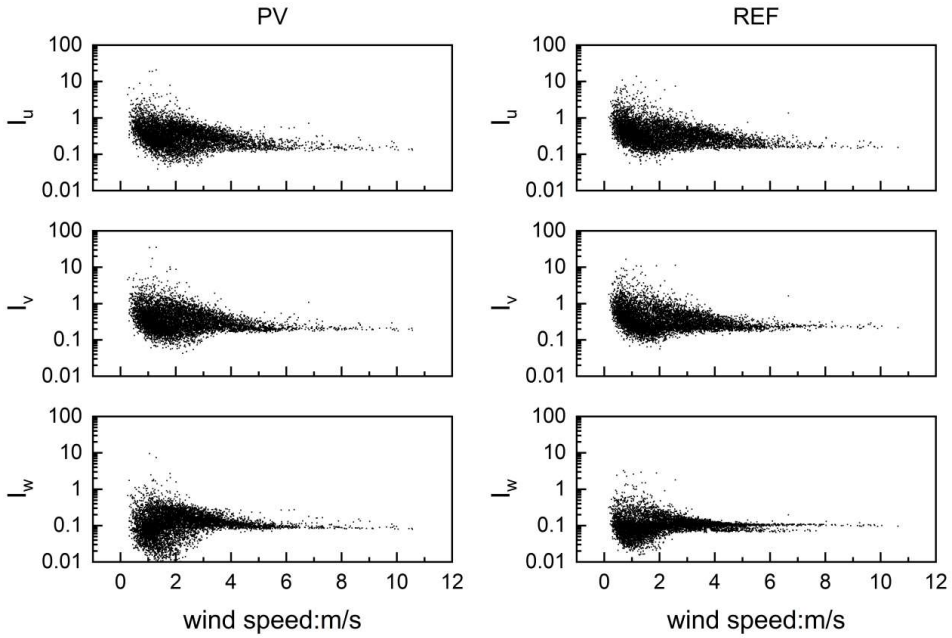

Figure 5. Relationship between turbulence intensity and wind speed.

Preprints (www.preprints.org) | NOT PEER-REVIEWED | Posted: 24 November 2020 doi:10.20944/preprints202011.0608.v1

Turbulent kinetic energy (TKE,e) is an important indicator to measure the development and decline of turbulence, involving the transport of momentum, heat and water vapor in the boundary layer. The TKE increases rapidly after 8:00 during the daytime and reaches a maximum value around 16:00 but in the PV plant is lower than the reference site (Fig. 6(a)). It may be due to the large dissipation of turbulence kinetic energy in the PV plant. At night, the TKE of the PV plant and the reference site are basically the same, both maintained in the range of 0.2 to 0.4. From the perspective of the relationship between the TKE and wind speed (Fig. 6(b) and Fig. 6(c)), when the wind speed is less than 4m/s, the TKE increases rapidly with the increase of wind speed. When the wind speed is greater than 4m/s, the TKE in the PV plant and the reference site is basically stable, and the TKE in the PV plant is more discrete.

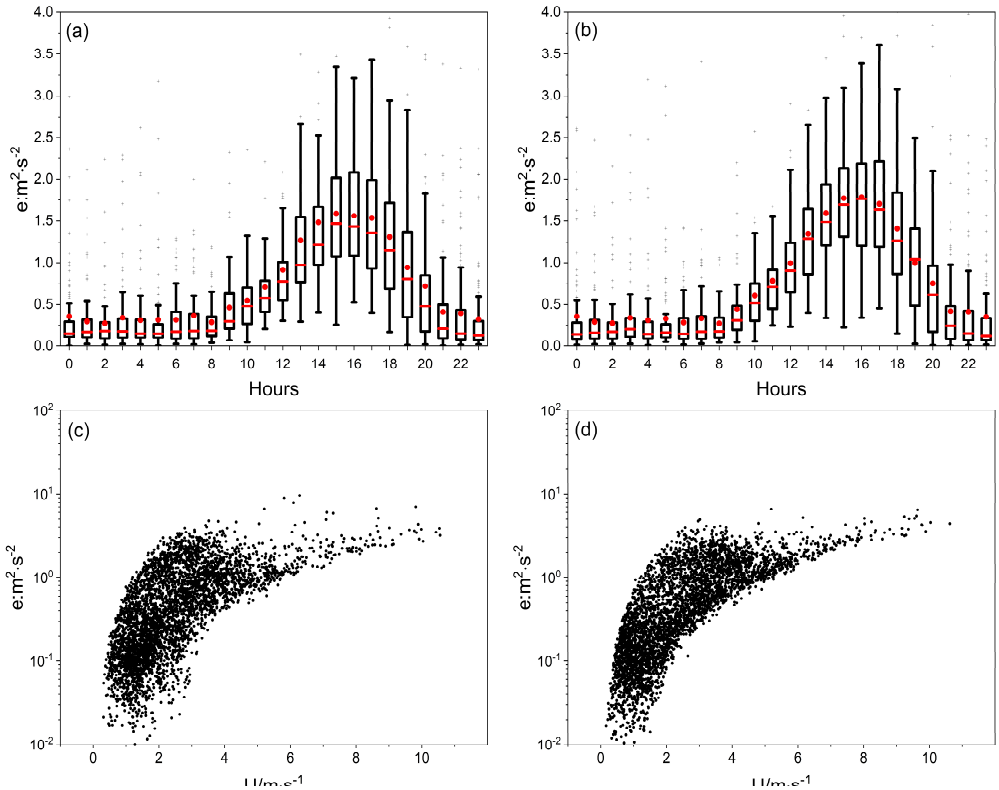

Figure 6. Diurnal variation of turbulent kinetic energy e in the PV plant (a) and the reference site (b). The height of the box shows the range from 25th to 75th percentile. The horizontal red line inside the box and solid red dot denote the median value and mean value respectively. The ends of the whiskers are drawn to 10th and 90th percentile values. the relationship between turbulent kinetic energy and wind speed for the PV plant (c) and the reference site (d).

Preprints (www.preprints.org) | NOT PEER-REVIEWED | Posted: 24 November 2020 doi:10.20944/preprints202011.0608.v1

3.4 Momentum flux and heat flux

Diurnal variation of momentum flux shows in Figure 8 to invesgate the surface layer dynamics differece between the PV plant and the reference site. Momentum is positive in the whole day and shows obvious diurnal variation in both sites. The momentum fluxes during the daytime are higher than that of the nighttime and the high values of momentum fluxes are related to the strong convective turbulence and highly unstable conditions. PV panels enhance the vertical interaction with the airflow above the panels, hence the wind shear as the main contributor for mechanical turbulance is stronger in the PV plant than the reference site. The peak daytime momentum fluxes in the PV plant and the reference site are 0.17 and 0.14$kg \cdot m^{-1} \cdot s^{-2}$ respectively. The low momentum flux at night is associated with the weak development of turbulence and the momentum flux in the PV plant is slightly higher than that of the reference site in the late night.

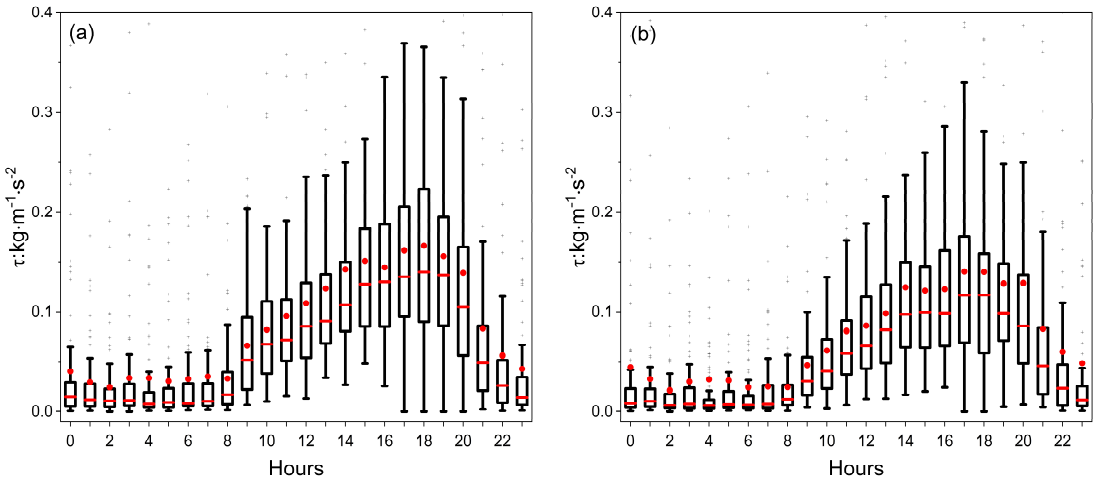

Figure 7. Diurnal variation of momentum flux in the PV plant (a) and the reference site (b). The height of the box shows the range from 25th to 75th percentile. The horizontal red line inside the box and solid red dot denote the median value and mean value respectively. The ends of the whiskers are drawn to 10th and 90th percentile values.

The vertical heat as a measure of the surface buoyancy reflects the intensity of heat and water exchange between earth and near surface atmosphere. Figure 9 shows the diurnal variation of sensible and latent heat flux in the PV plant (Figure 9(a)) and the reference site (Figure 9(b)). The positive value from 9:00 to 20:00 during the daytime indicate upward sensible heat flux from surface to the atmosphere due to solar radiation heating for the surface. The maximum sensible heat fluxes are observed at about 15:00 with values of 246.3 and 175W/m^2 for the PV plant and the reference site respectively. Compared to the reference site, the lower heat capacity and increased surface area in the PV plant generate stronger convective conditions, resulting higher sensible heat flux. The minimum heat fluxes are observed during 7:00~8:00 indicating near neutral conditions during the early morning. The negative value in night indicate downward sensible heat flux from loft atmosphere to surface caused by surface radiative cooling. With regear to the latent heat flux, the observed peak values are 52.4 and 98.9 W/m^2 at 14:00 for the PV plant and the reference site respectively. The wind resistance and shielding effect of PV panels in the PV plant bring about less evaporation compared with the reference site. The positive latent heat flux at night is close to zero, which indicates that there is weak evaporation at night in both sites.

Preprints (www.preprints.org) | NOT PEER-REVIEWED | Posted: 24 November 2020 doi:10.20944/preprints202011.0608.v1

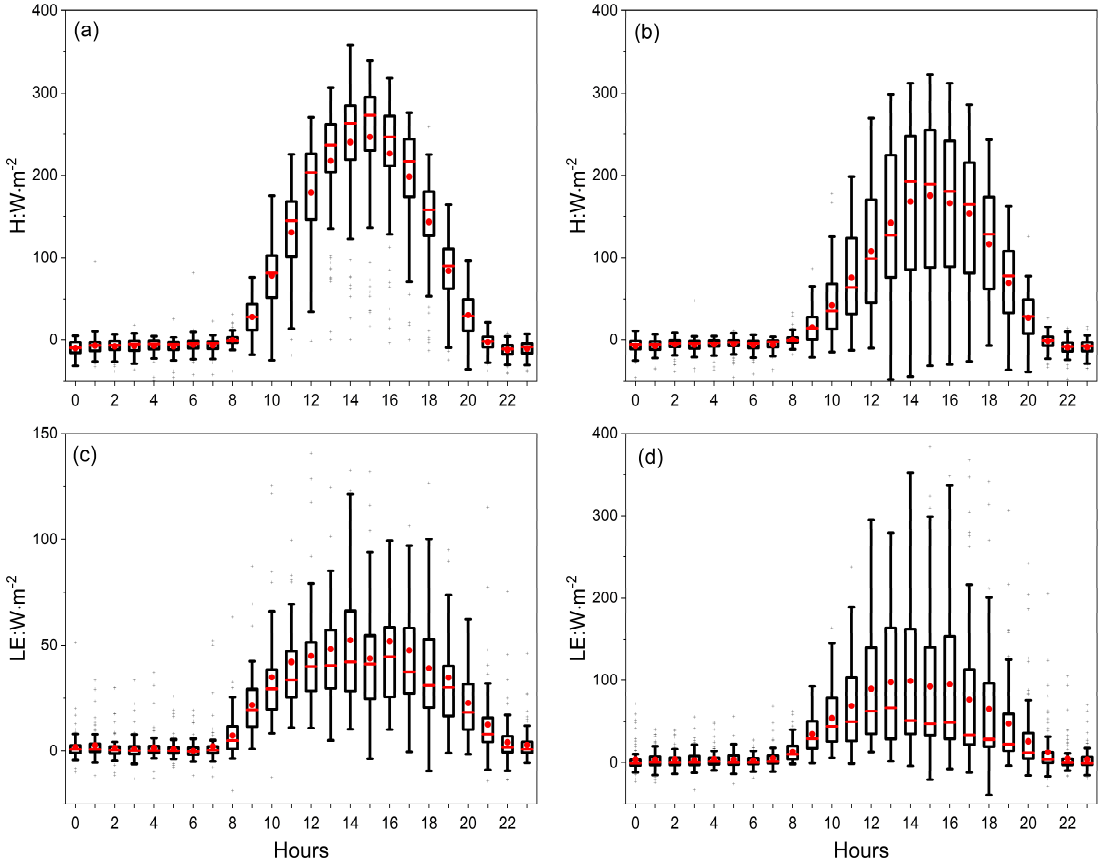

Figure 8. Diurnal variation of sensible heat flux (H,W · m^{-2}) in the PV plant (a) and the reference site (b) and the latent heat flux (LE,W · m^{-2}) in the PV plant (c) and the reference site (d). The height of the box shows the range from 25th to 75th percentile. The horizontal red line inside the box and solid red dot denote the median value and mean value respectively. The ends of the whiskers are drawn to 10th and 90th percentile values.

3.5. The relationship between turbulence variance and stability

The normalized standard deviation of the wind speed component that describes the relationship between the near-surface variance and the flux, and represents the overall characteristics of turbulence are applied to a variety of atmospheric diffusion modes. These relationships depend on the spatial and temporal in-homogeneities of the atmospheric motions and that they are also dependent on the atmospheric stability [39]. Additional, turbulent intensity relationships may may be affected by geographical location, dynamic and the thermal characteristics of the atmosphere [40].

Here we fitted the relationship between σ_u/u_*, σ_v/u_*, σ_w/u_* and zL respectively for the PV plant and the reference site according to the formula (11), and the best similarity coefficients are shown in Table 1. In the near neutral range ($-0.1 < \frac{z}{L} < 0.1$), turbulence is assumed to be isotropic and turbulent motion is decoupled from the surface, the statistical characteristics of turbulence are independent of height and tend to be a constant. Under unstable conditions, the relationship between the horizontal and vertical wind speed normalized deviation and stability can conform to the 1/3 square law for the PV site and the reference site (Figure 9). Compared with the horizontal velocity, the vertical velocity variance has better similarity, and the dispersion of scatters are small, the main reason is that the energy of vertical movement is buoyancy; and the wind velocity variance similarity of the three directions of the reference site is better than that of the PV plant, especially in the u and v directions, may be caused by the difference between the PV plant and reference site. Under stable conditions, the wind speed variance of the PV plant and the reference site can also basically meet the

Preprints (www.preprints.org) | NOT PEER-REVIEWED | Posted: 24 November 2020 doi:10.20944/preprints202011.0608.v1

similarity theory, but the dispersion of scatters are greater than that of the unstable conditions. The similarity of the wind speed variance of the PV plant is better than that of the reference site, especially in the w direction.

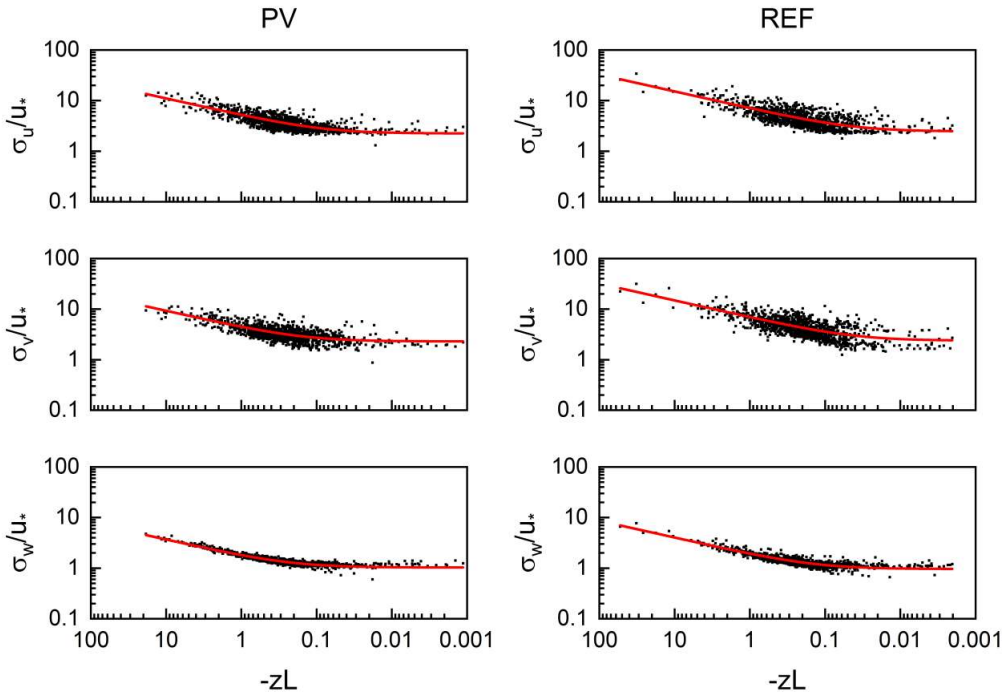

Figure 9. Normalized standard deviation of longitudinal wind velocity (σ_u/u_*), lateral wind velocity (σ_v/u_*) and vertical wind velocity σ_w/u_* for unstable stratification conditions at the PV plant (left) and the reference site (right) from June to October 2019. The red solid line represents the empirical relations applied to the observed data.

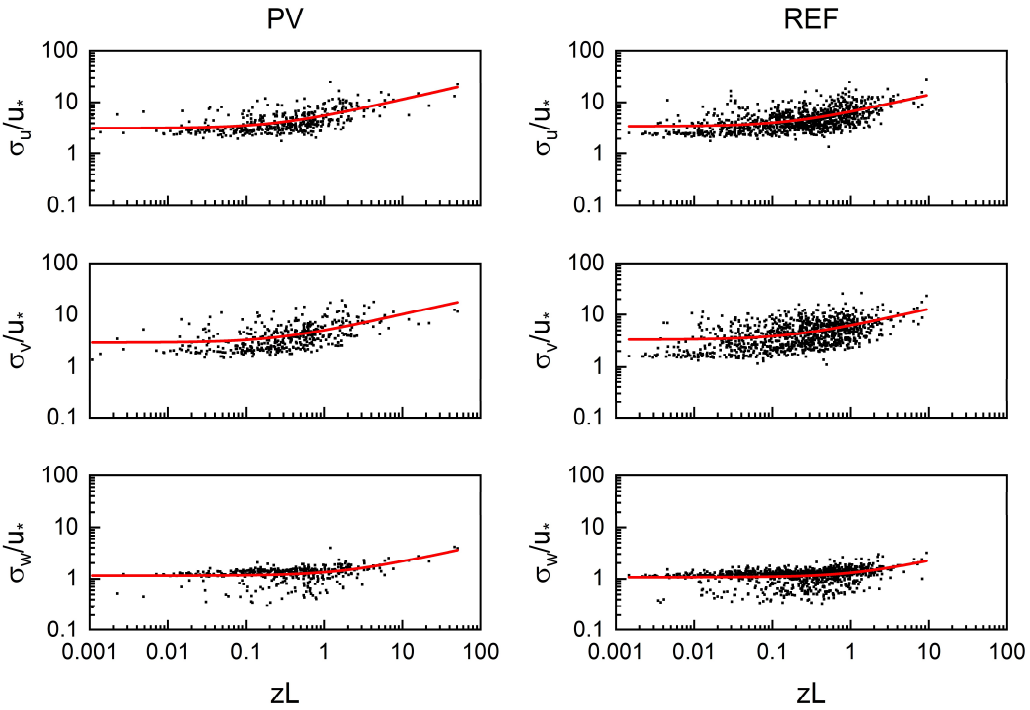

Figure 10. The same as Figure. 9 under stable stratification conditions.

Preprints (www.preprints.org) | NOT PEER-REVIEWED | Posted: 24 November 2020 doi:10.20944/preprints202011.0608.v1

Table 1. Optimal similarity function coefficients for fitting normalized standard deviation of longitudinal wind velocity (σ_u/u_*), lateral wind velocity (σ_v/u_*), vertical wind velocity σ_w/u_* under unstable and stable stratification conditions for the observed data from June to October 2019.

	Unstable						Stable					
	PV			REF			PV			REF		
	a	b	R^2	a	b	R^2	a	b	R^2	a	b	R^2
σ_u/u_*	2.24	11.97	0.67	3.01	8.67	0.59	3.16	3.73	0.41	3.50	6.05	0.30
σ_v/u_*	2.30	6.50	0.58	3.11	7.4	0.53	2.1	3.52	0.30	3.31	5.7	0.20
σ_w/u_*	1.03	4.51	0.92	1.01	5.42	0.89	1.12	0.67	0.30	1.08	0.78	0.15

4. Conclusion

To explore the impact of PV panels on turbulence, the observation of turbulence characteristics in the PV plant and the reference site over gobi area from June to October 2019 in Wujiaqu in Xinjiang were compared. As far as we know, this is the first time to explore the atmospheric turbulence characteristics of utility-scale PV plant. Results indicate that in the study region, near surface boundary layer is more unstable during the daytime while is more stable at the night in the PV plant than the reference site. The turbulence intensity in the longitudinal direction (I_u) of the PV plant is higher than the reference site and in the lateral direction (I_v) is opposite during the daytime, at night the I_u and I_v of the PV plant is lower than the reference site. The turbulence intensity in the vertical direction (I_w) of the PV plant is higher than the reference site especially during the daytime. The turbulent kinetic energy of the PV plant during the daytime is lower than the reference site.

As regard to the turbulent fluxes, the momentum which is dominated by mechanical turbulence in the PV plant is higher than the reference site, especially during the daytime. Compared to the reference site, the lower heat capacity and increased surface area of the PV panels generate stronger convective conditions, resulting higher sensible heat flux while the latent heat flux is reduced due to the wind resistance and shielding effect of PV panels in the PV plant.

Site specific turbulent intensity relationships were developed for the PV plant and the reference site by analyzing wind components as a function of stability parameter (z/L). The turbulent components of wind followed 1/3 power law in the unstable conditions and stable conditions in the PV plant and the reference site. Comparison of the derived relationships of the PV plant with the reference site indicates that the turbulent intensity for vertical winds at the PV plant is relatively strong especially in the unstable conditions.

Declaration of Competing Interest

The authors declare that they have no known competing financial interests or personal relationships that could have appeared to influence the work reported in this paper.

Acknowledgment

This work is financially supported by the National Key Research and Development Program of China (2018YFB1502800), the National Natural Science Foundation of China (41805085).

References

1. Panwar, N. L.; Kaushik, S. C.; Kothari, S., Role of renewable energy sources in environmental protection: A review. *Renew. Sust. Energ. Rev.* **2011,** 15, (3), 1513-1524.
2. De Marcoa, A., Petrosillo, I., Semeraro, T., Pasimeni, M.R., Aretano, R., Zurlini, G., The contribution of Utility-Scale Solar Energy to the global climate regulation and its effects on local ecosystem services. Glob. Ecol. Conserv. 2014, 2, 324-337.
3. Haegel, N.M., Margolis, R., Buonassisi, T., Feldman, D., Froitzheim, A., Garabedian, R., Green,

Preprints (www.preprints.org) | NOT PEER-REVIEWED | Posted: 24 November 2020 doi:10.20944/preprints202011.0608.v1

M., Glunz, S., Henning, H.M., Holder, B., Kaizuka, I., Kroposki, B., Matsubara, K., Niki, S., Sakurai, K., Schindler, R.A., Tumas, W., Weber, E.R., Wilson, G., Woodhouse, M., Kurtz, S., Terawatt-scale photovoltaics: Trajectories and challenges, *Science* **2017**,356,(6334) 141-143.

4. C. Breyer, D. Bogdanov, A. Gulagi, A. Aghahosseini, L. Barbosa, O. Koskinen, M. Barasa, U. Caldera, S. Afanasyeva, M. Child, J. Farfan, P. Vainikka, On the role of solar photovoltaics in global energy transition scenarios, *Prog. Photovoltaics* 25(8) (2017) 727-745.
5. J.J. Burkhardt, III, G. Heath, E. Cohen, Life Cycle Greenhouse Gas Emissions of Trough and Tower Concentrating Solar Power Electricity Generation, Journal of Industrial Ecology 16 (2012) S93-S109.
6. S. Ravi, D.B. Lobell, C.B. Field, Tradeoffs and Synergies between Biofuel Production and Large Solar Infrastructure in Deserts, Environmental Science & Technology 48(5) (2014) 3021-3030.
7. Pielke, R. A.; Marland, G.; Betts, R. A.; Chase, T. N.; Eastman, J. L.; Niles, J. O.; Niyogi, D. D. S.; Running, S. W., The influence of land-use change and landscape dynamics on the climate system: relevance to climate-change policy beyond the radiative effect of greenhouse gases. Philos. Trans. R. Soc. Lond. Ser. A-Math. Phys. Eng. Sci. 2002, 360, (1797), 1705-1719.
8. Bonan, G. B., Forests and climate change: Forcings, feedbacks, and the climate benefits of forests. *Science* **2008,** 320, (5882), 1444-1449.
9. Barron-Gafford, G. A.; Minor, R. L.; Allen, N. A.; Cronin, A. D.; Brooks, A. E.; Pavao-Zuckerman, M. A., The Photovoltaic Heat Island Effect: Larger solar power plants increase local temperatures. *Scientific Reports* **2016,** 6, (1), 35070.
10. Chang, R.; Shen, Y.; Luo, Y.; Wang, B.; Yang, Z.; Guo, P., Observed surface radiation and temperature impacts from the large-scale deployment of photovoltaics in the barren area of Gonghe, China. *Renewable Energy* **2018,** 118, 131-137.
11. Yang, L.; Gao, X.; Lv, F.; Hui, X.; Ma, L.; Hou, X., Study on the local climatic effects of large photovoltaic solar farms in desert areas. *Solar Energy* **2017,** 144, 244-253.
12. A. Armstrong, N.J. Ostle, J. Whitaker, Solar park microclimate and vegetation management effects on grassland carbon cycling, Environ. Res. Lett. 11(7) (2016) 11.
13. Hu, A. X.; Levis, S.; Meehl, G. A.; Han, W. Q.; Washington, W. M.; Oleson, K. W.; van Ruijven, B. J.; He, M. Q.; Strand, W. G., Impact of solar panels on global climate. *Nat. Clim. Chang.* **2016,** 6, (3), 290-294.
14. Li, Y.; Kalnay, E.; Motesharrei, S.; Rivas, J.; Kucharski, F.; Kirk-Davidoff, D.; Bach, E.; Zeng, N., Climate model shows large-scale wind and solar farms in the Sahara increase rain and vegetation. *Science* **2018,** 361, (6406), 1019-1022.
15. Broadbent, A. M.; Krayenhoff, E. S.; Georgescu, M.; Sailor, D. J., The Observed Effects of Utility-Scale Photovoltaics on Near-Surface Air Temperature and Energy Balance. *J. Appl. Meteorol. Climatol.* **2019,** 58, (5), 989-1006.
16. Foken, T., Micrometeorology. 2008, Springer, New York, p 308
17. Stull, R.B., An introduction to boundary layer meteorology.1988, Kluwer,Dordrecht, p 680
18. K. Prasad, C.V. Srinivas, A.B. Singh, C.V. Naidu, R. Baskaran, B. Venkatraman, Turbulence characteristics of surface boundary layer over the Kalpakkam tropical coastal station, India, Meteorol. Atmos. Phys. 131(4) (2019) 827-843.
19. Dyer, A. J.; Garratt, J. R.; Francey, R. J.; McIlroy, I. C.; Bacon, N. E.; Hyson, P.; Bradley, E. F.;

Preprints (www.preprints.org) | NOT PEER-REVIEWED | Posted: 24 November 2020 doi:10.20944/preprints202011.0608.v1

Denmead, O. T.; Tsvang, L. R.; Volkov, Y. A.; Koprov, B. M.; Elagina, L. G.; Sahashi, K.; Monji, N.; Hanafusa, T.; Tsukamoto, O.; Frenzen, P.; Hicks, B. B.; Wesely, M.; Miyake, M.; Shaw, W., AN INTERNATIONAL TURBULENCE COMPARISON EXPERIMENT (ITCE 1976). *Boundary-Layer Meteorology* **1982,** 24, (2), 181-209.

20. Shuhua, L.; Jie, L.; Heping, L.; Fuming, L.; Jianhua, W.; .CHAN, J. C. L.; .CHEN, A. Y. S.; Fei, H.; Huizhi, L., Characteristics of Turbulence Spectra and Local Isotropy in EBEX-2000. *Chinese Journal of Atmospheric Sciences* **2005,** 29, (2), 213-224.
21. Panofsky, H. A. , et al. "The characteristics of turbulent velocity components in the surface layer under convective conditions." *Boundary Layer Meteorology* 11.3(1977):355-361.
22. B. Lange, S. Larsen, J. Hojstrup, R. Barthelmie, The influence of thermal effects on the wind speed profile of the coastalmarine boundary layer, Boundary-Layer Meteorology 112(3) (2004) 587-617.
23. Huizhi, L.; Zhongxiang, H., Turbulent Characteristics in the Surface Layer over Gerze Area in the Tibetan Plateau. *Chinese Journal of Atmospheric Sciences* **2000,** 24, (3), 289-300.
24. Yaoming, M.; Weiqiang, M.; Zeyong, H.; Maoshan, L.; Jiemin, W., Similarity Analysis of Atmospheric Turbulent Intensity over Grassland Surface of Qinghai-Xizang Plateau. *PLATEAU METEOROLOGY* **2002,** 21, (5), 514-517.
25. Huizhi, L.; Zhongxiang, H., Turbulent Statistical Characteristics over the Urban Surface. *Chinese Journal of Atmospheric Sciences* **2002,** 26, (2), 241-248.
26. Hedde, T.; Durand, P., TURBULENCE INTENSITIES AND BULK COEFFICIENTS IN THE SURFACE-LAYER ABOVE THE SEA. *Boundary-Layer Meteorology* **1994,** 71, (4), 415-432.
27. Huiwang, G.; Ming, G.; Renlei, W.; Yuhuan, X., Analysis of the Characteristics of the Atmospheric Turbulene Intensity and the Similarity of the Standard Deviations of Wind Velocity over the North Yellow Sea. *PE RIODICAL OF OCEAN UNIVERSIT Y OF CHINA* **2009,** 39, (04), 563-568+578.
28. Yaoming, M.; Jieming, W.; Wei, L.; Qingrong, Z.; Boqiang, M., The Study of the Characteristics of Both the Atmospheric Turbulence Structure and the Transfer in the Lower Layer of the Atmosphere above the Nansha Islands Area. **1997,** 21, (03), 102-110.
29. Wilson, K.; Goldstein, A.; Falge, E.; Aubinet, M.; Baldocchi, D.; Berbigier, P.; Bernhofer, C.; Ceulemans, R.; Dolman, H.; Field, C.; Grelle, A.; Ibrom, A.; Law, B. E.; Kowalski, A.; Meyers, T.; Moncrieff, J.; Monson, R.; Oechel, W.; Tenhunen, J.; Valentini, R.; Verma, S., Energy balance closure at FLUXNET sites. *Agricultural and Forest Meteorology* **2002,** 113, (1-4), 223-243.
30. Massman, W. J., A simple method for estimating frequency response corrections for eddy covariance systems. *Agricultural and Forest Meteorology* **2000,** 104, (3), 185-198.
31. Schotanus, P.; Nieuwstadt, F. T. M.; Debruin, H. A. R., TEMPERATURE-MEASUREMENT WITH A SONIC ANEMOMETER AND ITS APPLICATION TO HEAT AND MOISTURE FLUXES. *Boundary-Layer Meteorology* **1983,** 26, (1), 81-93.
32. Webb, E. K.; Pearman, G. I.; Leuning, R., CORRECTION OF FLUX MEASUREMENTS FOR DENSITY EFFECTS DUE TO HEAT AND WATER-VAPOR TRANSFER. *Q. J. R. Meteorol. Soc.* **1980,** 106, (447), 85-100.
33. RB, S., *Introduction to boundary layer meteorology*. Kluwer Academic Publishers: The Netherlands **1988**.
34. Rosenberg, N.J., B.B. Blad, S.B. Verma. 1983. Microclimate: The Biological Environment, 2nd

Preprints (www.preprints.org) | NOT PEER-REVIEWED | Posted: 24 November 2020 doi:10.20944/preprints202011.0608.v1

ed. John Wiley & Son, New York, pp. 135.

35. Monin A S, A M Obukhov.Basic law s of turbulent mixing the atmospheric near the ground[M] .Akad Nauk .SSR, Geophiz Inst ,1954 .151 :1963 -1987
36. Qiang, Z.; J, Z.; T, Y., Interaction of aerodynamic roughness length and windflow conditions and its parameterization over vegetation surface. *Chin Sci Bull* **2012,** 13, 97-105.
37. Prueger, J. H.; Kustas, W. P.; Hipps, L. E.; Hatfield, J. L., Aerodynamic parameters and sensible heat flux estimates for a semi-arid ecosystem. *J. Arid. Environ.* **2004,** 57, (1), 87-100.
38. Yinhuan, A.; Shihua, L.; bo, H.; Zhaoguo, L., Analysis on Micrometeorology Characteristics in Surface Layer over Badan Jaran Desert in Summer *PLATEAU METEOROLOGY* **2013,** 32, (06), 1682-1691.
39. McBean GA (1971) The variations of the statistics of wind, temperature and humidity fluctuations with stability. Bound Layer Meteorol, 1:438 – 457.
40. Singha A, Sadr R (2012) Characteristics of surface layer turbulence in coastal area of Qatar. Environ Fluid Mech 12(6):515 – 531